Cardiovascular Research (2012) **94**, 408–417
doi:10.1093/cvr/cvs117

Down-regulation of OPA1 alters mouse mitochondrial morphology, PTP function, and cardiac adaptation to pressure overload

Jerome Piquereau[1,2†], Fanny Caffin[1,2†], Marta Novotova[3], Alexandre Prola[1,2], Anne Garnier[1,2], Philippe Mateo[1,2], Dominique Fortin[1,2], Le Ha Huynh[1,2], Valérie Nicolas[2], Marcel V. Alavi[4], Catherine Brenner[1,2], Renée Ventura-Clapier[1,2], Vladimir Veksler[1,2], and Frédéric Joubert[1,2*]

[1]INSERM, U-769, Faculté de Pharmacie, Université Paris-Sud, 5 rue J-B Clément, F-92296 Châtenay-Malabry, France; [2]Univ Paris-Sud, IFR141, F-92296 Châtenay-Malabry, France; [3]Institute of Molecular Physiology and Genetics, Slovak Academy of Sciences, Bratislava, Slovak Republic; and [4]Department of Biologie, Institut für Zoologie, Johannes-Gutenberg Universität Mainz, Mainz, Germany

Received 20 October 2011; revised 29 February 2012; accepted 6 March 2012; online publish-ahead-of-print 8 March 2012

Time for primary review: 25 days

Aims The optic atrophy 1 (OPA1) protein is an essential protein involved in the fusion of the mitochondrial inner membrane. Despite its high level of expression, the role of OPA1 in the heart is largely unknown. We investigated the role of this protein in $Opa1^{+/-}$ mice, having a 50% reduction in OPA1 protein expression in cardiac tissue.

Methods and results In mutant mice, cardiac function assessed by echocardiography was not significantly different from that of the $Opa1^{+/+}$. Electron and fluorescence microscopy revealed altered morphology of the $Opa1^{+/-}$ mice mitochondrial network; unexpectedly, mitochondria were larger with the presence of clusters of fused mitochondria and altered cristae. In permeabilized mutant ventricular fibres, mitochondrial functional properties were maintained, but direct energy channelling between mitochondria and myofilaments was weakened. Importantly, the mitochondrial permeability transition pore (PTP) opening in isolated permeabilized cardiomyocytes and in isolated mitochondria was significantly less sensitive to mitochondrial calcium accumulation. Finally, 6 weeks after transversal aortic constriction, $Opa1^{+/-}$ hearts demonstrated hypertrophy almost two-fold higher ($P < 0.01$) than in wild-type mice with altered ejection fraction (decrease in 43 vs. 22% in $Opa1^{+/+}$ mice, $P < 0.05$).

Conclusions These results suggest that, in adult cardiomyocytes, OPA1 plays an important role in mitochondrial morphology and PTP functioning. These properties may be critical for cardiac function under conditions of chronic pressure overload.

Keywords Cardiac energy metabolism • Mitochondria • Mitochondrial dynamics • Permeability transition pore • Hypertrophy

1. Introduction

Changes in mitochondrial morphology appear essential for the function or dysfunction of most tissues. Mitochondrial fusion and fission are highly regulated and tightly balanced processes. In mammalian cells, mitochondrial fission is regulated by dynamin-related protein 1 (DRP1) and its receptor FIS1 (fission-mediator protein 1) (for review, see Liesa *et al.*[1]). In turn, mitochondrial fusion is mediated by two mitofusins (MFN1 and MFN2),[2] which are involved in outer membrane fusion, and OPA1 (optic atrophic type 1 protein), which is closely linked to the inner membrane.[3] Mutations of genes encoding these proteins lead to severe diseases, especially neurological disorders, such as Charcot–Marie–Tooth disease type 2A for *Mfn2* or autosomal dominant inherited optic atrophy (DOA) for *Opa1* mutations.[4–7]

OPA1 is a ubiquitously expressed protein[4,8] and its level is particularly up-regulated in the heart. Because OPA1 is involved in the regulation of the dynamics of mitochondria that occupy ~30% of the

† Both authors contributed equally to this work.

* Corresponding author. Tel: +33 1 46 83 52 48; fax: +33 1 46 83 54 75, Email: frederic.joubert@u-psud.fr

cardiac cell volume, OPA1 may play a role in cardiac energy metabolism. We have previously shown that the energetic transfer between mitochondria and energy-consumers performed by direct adenylic nucleotide channelling (DANC)[9] is closely related to the cell architecture and mitochondrial network.[10,11] Finally, because decreased mitochondrial content and mitochondrial fragmentation are key features of cardiac diseases,[12,13] alterations of mitochondrial morphology could be of major pathophysiological relevance.[14] Indeed, a heterozygous mutation of *Opa1* in *Drosophila*[15] is associated with decreased heart rate and cardiac arrhythmia, suggesting that a loss of OPA1 could induce cardiac function abnormalities. Heart tube-specific knockdown of Opa1 also induces heart tube dilation with profound contractile impairment.[16] In heart failure, a decrease in OPA1 protein content associated with mitochondrial fragmentation[17] has been shown but the exact role of OPA1 depletion in the adult mammalian heart has not yet been assessed.

Recently, a mouse model carrying a splice mutation in the *Opa1* gene leading to haploinsufficiency was described.[18,19] While homozygous mutants die *in utero*, heterozygous mutants are viable but exhibit an age-dependent loss of retinal ganglion cells (characteristic of DOA) with a disorganization of the mitochondrial cristae. This mouse model thus appears to be of great interest in studying the role of OPA1 in mitochondrial morphology, organization, and function in the heart.

2. Methods

Supplementary methods are available in the Supplementary material online.

2.1 Animals

The B6;C3-*Opa1*$^{329-355del}$ mouse line (herein referred to as *Opa1*$^{+/-}$) has been described in details before.[18–20] Basal cardiac phenotype was determined in 6-month-old male mice, while 10-week-old mice were submitted to transverse aortic constriction (TAC) to estimate the ability of mutated mouse hearts to adapt to pathological stress. Anaesthesia was induced by ip injection of ketamine (50 mg/kg) and xylazine (8 mg/kg). Aortic stenosis was induced by placing a silk suture around the aorta after thoracic incision. Age-matched controls underwent the same procedure without placement of suture. Mice were studied 6 weeks after surgery. All mice were anaesthetized by ip injection of pentobarbital (200 mg/kg). The depth of anaesthesia was checked by toe pinch before the start of surgery. After thoracotomy, the animals' hearts were excised and rinsed in ice-cold calcium-free Krebs solution equilibrated with 95% O_2-5% CO_2.

All experiments were performed in conformity with the European Community guiding principles in the care and use of animals (Directive 2010/63/EU of the European Parliament). Authorizations to conduct animal experiments were obtained from the French Ministère de l'Agriculture, de la Pêche et de l'Alimentation (no. 92-284, 27 June 2007).

2.2 Biochemical analysis

Frozen tissues were used to measure activities of total creatine kinase (CK), citrate synthase (CS), and mitochondrial complex I by standard spectrophotometric assays as previously described.[11]

2.3 Echocardiography

Transthoracic echocardiography was performed using a 12 MHz transducer (Vivid 7, General Electric Healthcare) under 2.5% isoflurane gas anaesthesia. Two-dimensional-guided (2D) M-mode echocardiography was used to determine wall thickness and left ventricular (LV) chamber volume at systole and diastole and contractile parameters, such as fractional shortening (FS) or ejection fraction (EF).

2.4 Cardiomyocyte isolation

Retrograde heart perfusion according to the Langendorff method was performed to isolate cardiomyocytes as previously shown.[21] The cells were plated onto dishes coated with laminin and were kept at room temperature for 2 h.

2.5 Morphological description of mitochondrial network by fluorescence microscopy

Freshly isolated cardiomyocytes were incubated for 45 min at room temperature with 500 nM Mito-Tracker Orange dye to label mitochondria and with 1 μM calcein to estimate global cell volume (Invitrogen). Three-dimensional reconstruction was performed using the IMARIS software (Bitplane Company, Zurich, Switzerland).

2.6 Electron microscopy

Samples of LV papillary muscle from 6-month-old mice were prepared for electron microscopy as previously described.[10]

2.7 Analysis of *in situ* mitochondrial function

Mitochondrial respiration was studied *in situ* in saponin-permeabilized fibres, as previously described.[22] Fibres were exposed to increasing (ADP), and the ADP-stimulated respiration above basal oxygen consumption (V_0) was plotted to determine the apparent K_m for ADP and the maximal respiration rate (V_{max}). The acceptor control ratio (ACR), an index of the oxidation–phosphorylation coupling, was calculated as V_{max}/V_0 in the presence of glutamate/malate as substrates.

2.8 Estimation of energy transfer to sarcoplasmic reticulum and myofilaments

For measurements of sarcoplasmic reticulum (SR) and myofibrillar function, papillary muscle fibres were dissected and permeabilized for 30 min in saponin (50 μg/mL), as previously described.[9] The contribution of the energetic transfer system, the CK system, and the DANC to the provision of ATP for SR ATPase (SERCA) function, was estimated by measuring the SR calcium content in saponin-permeabilized fibres after loading under various energetic conditions, as previously described.[10,11] The pMgATP/rigour tension relation was used to studying the ability of the different energetic systems to supply ATP for myosin ATPase.[23]

2.9 Mitochondrial permeability transition pore experiments

For permeability transition pore (PTP) experiments, fresh cardiomyocytes were co-loaded in culture medium with 5 μM Rhod-2 and 1 μM calcein (Invitrogen) for 45 min at room temperature and washed with culture medium solution.

In additional experiments, mitochondria from *Opa1*$^{+/+}$ and *Opa1*$^{+/-}$ were isolated according to[24]. Swelling and depolarization of mitochondria were monitored after Ca^{2+} addition as described in[25].

2.10 Quantitative RT–PCR

RNA was extracted with Trizol reagent (Invitrogen), and transcribed into cDNA with the High Capacity cDNA Reverse Transcription Kit (Applied Biosystems, France). Real-time PCR was performed using TaqMan low density array technology (see Supplementary material online).

2.11 Statistical analysis

Values are expressed as means ± SEM. The statistical significance of the difference between the *Opa1*$^{+/+}$ and *Opa1*$^{+/-}$ groups was estimated by Student's *t*-test, and when necessary by two-way ANOVA using the Newman–Keuls *post hoc* test. Values of $P < 0.05$ were considered significant.

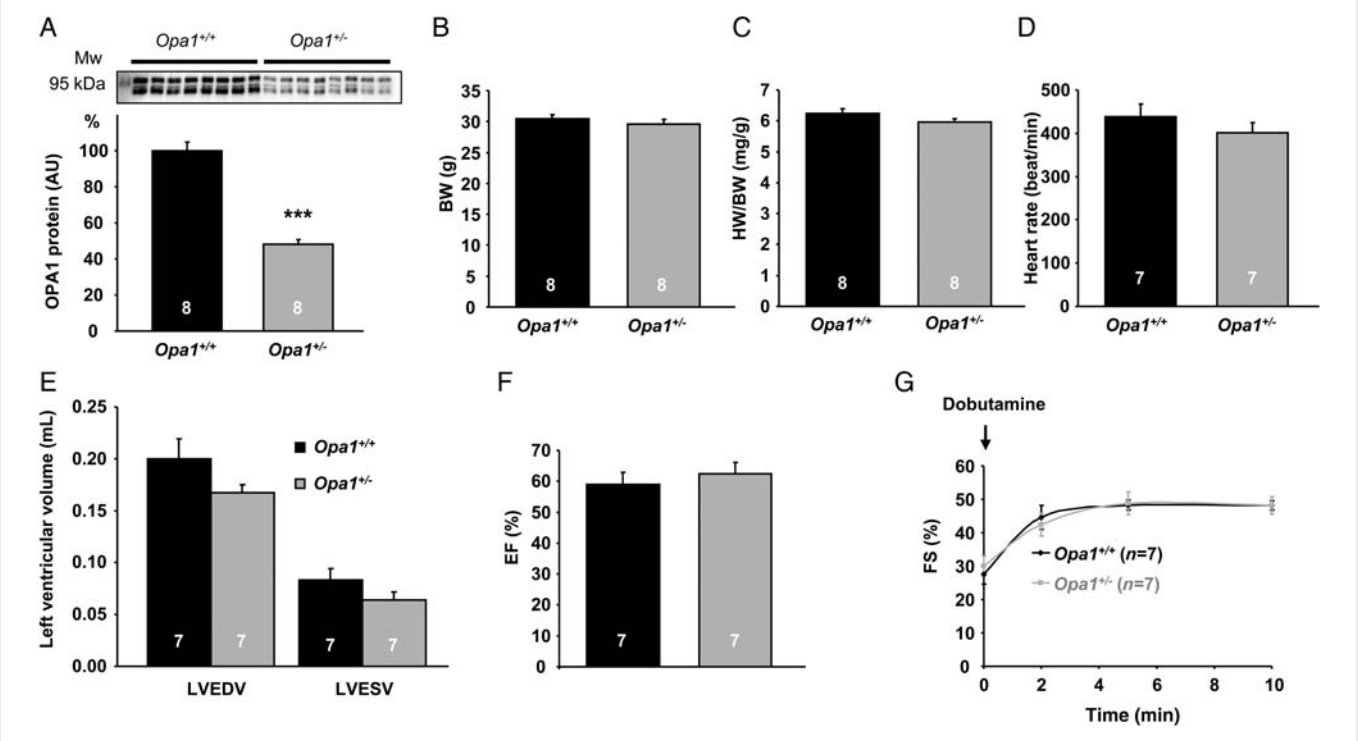

Figure 1 Anatomical characteristics and cardiac function of 6-month-old $Opa1^{+/+}$ and $Opa1^{+/-}$ mice. (*A*) Western blot analysis of OPA1 protein. Upper panel: a representative original recording. Lower panel: mean values of OPA1 protein. $^{***}P < 0.001$ vs. $Opa1^{+/+}$. (*B*) Body weight (BW). (*C*) Heart weight to body weight (HW/BW) ratio. (*D*) Heart rate. (*E*) LV end-diastolic volume (LVEDV) and LV end-systolic volume (LVESV). (*F*) LV ejection fraction (EF). (*G*) LV fractional shortening (FS) after dobutamine stimulation.

3. Results

3.1 Anatomical characteristics and heart function

The heterozygous mutation in *Opa1* resulted in a ~50% reduction in OPA1 protein (*Figure 1A*) in line with previous results.[18] Six-month-old $Opa1^{+/-}$ mice displayed normal body weight and growth (*Figure 1B*). There was no difference in heart weight between $Opa1^{+/+}$ and $Opa1^{+/-}$ mice (*Figure 1C*). The heart rate, LV end-diastolic and LV end-systolic volumes, as well as EF assessed by echocardiography, were normal in $Opa1^{+/-}$ (*Figure 1D–F*). Similarly, the contractile reserve, revealed by infusion of dobutamine (a β-adrenergic receptor agonist), was not compromised in $Opa1^{+/-}$ mice (*Figure 1G*). Thus, in adult $Opa1^{+/-}$ mice, cardiac function was normal and able to respond normally to an acute stimulation.

3.2 Cardiomyocyte ultrastructure and mitochondrial network organization

Compared with $Opa1^{+/+}$, the mitochondrial network in $Opa1^{+/-}$ cardiomyocytes appeared to be more heterogeneous, with larger mitochondria and/or an increase in the number of mitochondrial clusters and an increase in volume dispersion (*Figure 2A*). IMARIS analysis revealed that $Opa1^{+/-}$ cardiomyocyte and global mitochondrial volumes were identical to control (*Figure 2B* and *C*). However, the distribution of mitochondrial volumes was shifted, with an increase in the percentage of large mitochondria ($P < 0.01$) and a decrease in the proportion of small mitochondria in $Opa1^{+/-}$ cardiomyocytes ($P < 0.05$) (*Figure 2E*). This is consistent with a decreased number of mitochondria per cell (*Figure 2D*). These results show that OPA1 partial deficiency affects the mitochondrial network morphology of adult cardiomyocytes by modifying the distribution and morphology of individual mitochondria rather than the global mitochondrial volume.

To describe more precisely the structure of $Opa1^{+/-}$ mitochondria, we performed detailed electron microscopic analysis of cardiac tissue. Compared with $Opa1^{+/+}$ hearts where mitochondria form regular rows that extended along myofibrils (*Figure 3A* and *B*, upper panel; and *A*, lower panel), the arrangement of mitochondria in $Opa1^{+/-}$ cardiomyocytes was mostly irregular (*Figure 3C*, upper panel), with clusters of mitochondria (*Figure 3C* and *D*, upper panel) and high variability in size and shape (*Figure 3B*, upper panel), which was clearly visible in transverse sections (*Figure 3D*, upper panel). The mitochondrial cristae of $Opa1^{+/-}$ formed semi-circular areas alternating with areas of disintegrated cristae within the same mitochondrion and unusual areas displaying slight spatial deformation of cristae inside mitochondria (*Figure 3B*, lower panel). Other mitochondria displayed fragmented cristae (*Figure 3C*, lower panel) together with foci in the matrix that were devoid of cristae and the formation of free spaces between the outer and inner mitochondrial membranes (*Figure 3C*, lower panel). Typically, the presence of large mitochondria was accompanied by the presence of dark material that coincided with the disappearance of the outer and inner mitochondrial membranes. These defects may represent the sites where abnormal non-completed mitochondrial fusion took place due to the deficiency in OPA1 (*Figure 3D*, lower panel).

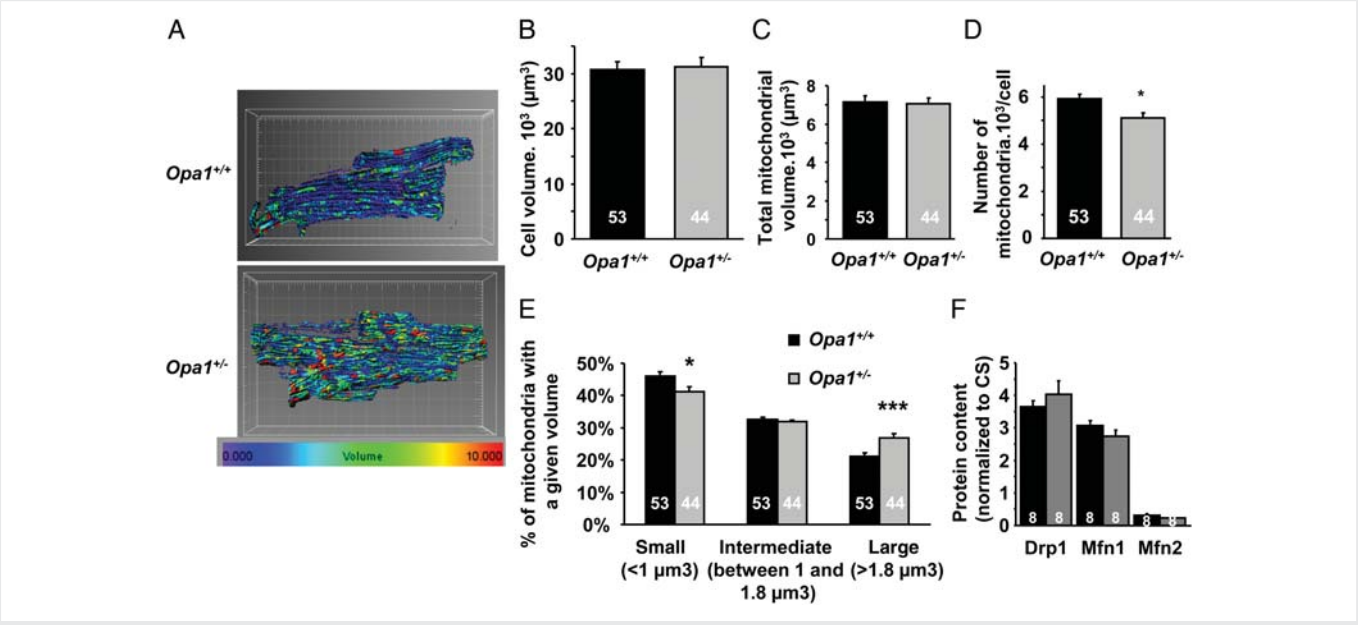

Figure 2 Morphological description of the mitochondrial network. (*A*) Representative pictures obtained with Mito-Tracker orange and IMARIS software. Each mitochondrion is identified by a colour in accordance with its volume (the smallest mitochondria are blue and the largest are red). (*B*) Cell volume measured by calcein loading and IMARIS analysis. (*C*) Total mitochondrial volume quantified by IMARIS. (*D*) The number of mitochondria per cell. (*E*) Percentage of mitochondrial size categories. (*F*) Level of proteins involved in mitochondrial dynamics (Drp1, Mfn1, Mfn2) in $Opa1^{+/+}$ and $Opa1^{+/-}$ cardiac tissue estimated by Western blot analysis (normalized to citrate synthase level). $^{*}P < 0.05$; $^{***}P < 0.001$ vs. $Opa1^{+/+}$.

We confirmed by EM analysis an increase in the mean surface of individual mitochondria (Supplementary material online, *Figure S1*), showing that the observed larger mitochondria observed in fluorescence were not clusters of small mitochondria, and that OPA1 partial deletion in the heart results in large mitochondria with incomplete fusion of inner membranes.

We also determined whether partial OPA1 deletion was accompanied by compensatory responses of other proteins involved in mitochondrial dynamics. Gene expression of *Drp1*, *Fis1*, *Mfn1*, and *Mfn2* was similar between control and mutant mice (Supplementary material online, *Figure S2*), showing no modification at the transcription level. Western blot experiments also revealed no compensation at the protein level (*Figure 2F*).

3.3 Oxidative capacity and energy transfer between mitochondria and myofilaments

We investigated whether the decrease of OPA1 expression could alter the intrinsic mitochondrial function. Basal and maximal respirations (when complex I, complex I and II, or complex II alone was activated) were not significantly different between the two groups (*Figure 4A*). Consequently, the coupling between oxidation and phosphorylation did not show any notable difference (*Figure 4B*). The sensitivity of mitochondrial respiration to ADP was estimated with and without creatine to study the coupling of oxidative phosphorylation with mitochondrial creatine kinase (mi-CK). The K_m for ADP without (K_{mADP}) and with creatine ($K_{mADP+Cr}$) was significantly lower in mutant mice (*Figure 4C*). However, the mi-CK functional efficacy assessed by $K_{mADP}/K_{mADP+Cr}$ was not significantly different between the two groups (2.6 ± 0.3 vs. 2.4 ± 0.6). Finally, when respiration was measured with octanoyl carnitine as the substrate, $Opa1^{+/-}$ cardiac mitochondria were less able to oxidize lipids than those of control mice (*Figure 4D*).

We also determined whether factors involved in mitochondrial biogenesis (PGC-1α and β, NRF, TFAM, ERRα, PPARα), glucose transport (GLUT1 and 4), and β-oxidation (CPT1, MCAD, LCAD) were modified. Except for a small decrease in NRF1 and a small increase in TFAM, none of the mRNA levels of these genes was modified (*Figure 4E*). Similarly, activities of CS, complex I, and total CK were not significantly different in $Opa1^{+/-}$ mice compared with $Opa1^{+/+}$ mice (*Figure 4F*). Finally, the level of oxidative stress was similar in $Opa1^{+/-}$ and $Opa1^{+/+}$ mice as estimated by the Oxyblot kit and by measuring aconitase/fumarase activities, Hsp60 protein level, and SOD and GPX1 mRNA levels (Supplementary material online, *Figure S3*). The same result was obtained for markers of autophagy which were not modified (Supplementary material online, *Figure S4*).

All these data demonstrate that down-regulation of OPA1 does not alter the respiratory capacity of mitochondria, oxidative stress status, or mitochondrial mass but may induce metabolic reprogramming at the level of substrate utilization.

Because energetic transfers, especially direct DANC between energy-producers (mitochondria) and energy-consumers (SERCA and ATPase of myofilaments), depend on the specific arrangement of the organelles in the cell, we measured energy transfer to SERCA in saponin-permeabilized ventricular fibres. The efficacy of each system (DANC or CK) was estimated relative to the efficacy of exogenous ATP only. The estimated maximal SR loading capacity under optimal energetic conditions in the presence of exogenous ATP, PCr, and working mitochondria was similar in both groups of mice. CK efficacy as well as DANC efficacy were also similar in $Opa1^{+/-}$ and $Opa1^{+/+}$ mice, suggesting that the adenine nucleotide channelling between mitochondria and SERCA was not altered by OPA1 deficiency (*Figure 4G*). EM images obtained in transversal

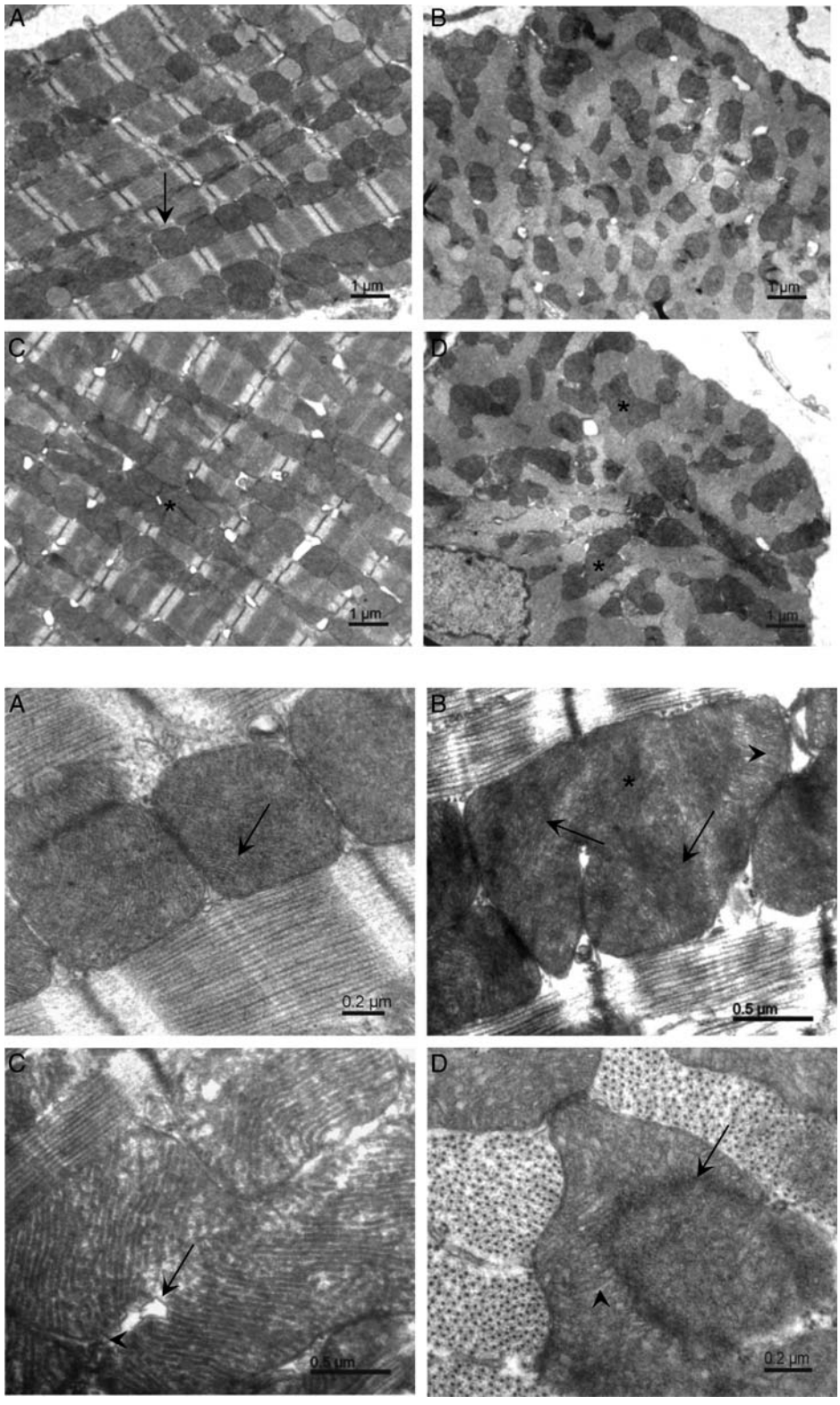

Figure 3 Electron micrographs of mitochondria in cardiomyocytes from *Opa1*$^{+/+}$ and *Opa1*$^{+/-}$ mice. Upper panel: longitudinal (*A*) and transverse (*B*) sections of *Opa1*$^{+/+}$ cardiomyocytes show individual mitochondria (arrow). Longitudinal (*C*) and transverse (*D*) sections of *Opa1*$^{+/-}$ cardiomyocytes demonstrate mitochondrial clusters (asterisks). Lower panel: (*A*) *Opa1*$^{+/+}$ cardiomyocytes. Cristae are homogeneously distributed in the mitochondria (arrow). (*B–D*) *Opa1*$^{+/-}$ cardiomyocytes showing enlarged mitochondria and incompletely fused cristae. (*B*) Cristae spreading in different directions (arrows); area of disintegrated cristae (asterisks); area of deformation of cristae (arrowhead). (*C*) Fragmented cristae (arrow); separation between inner and outer mitochondrial membranes (arrowhead). (*D*) Regions of incomplete mitochondrial fusion (arrow). Note that the peripheral part of the mitochondrion contains normal cristae (arrowhead).

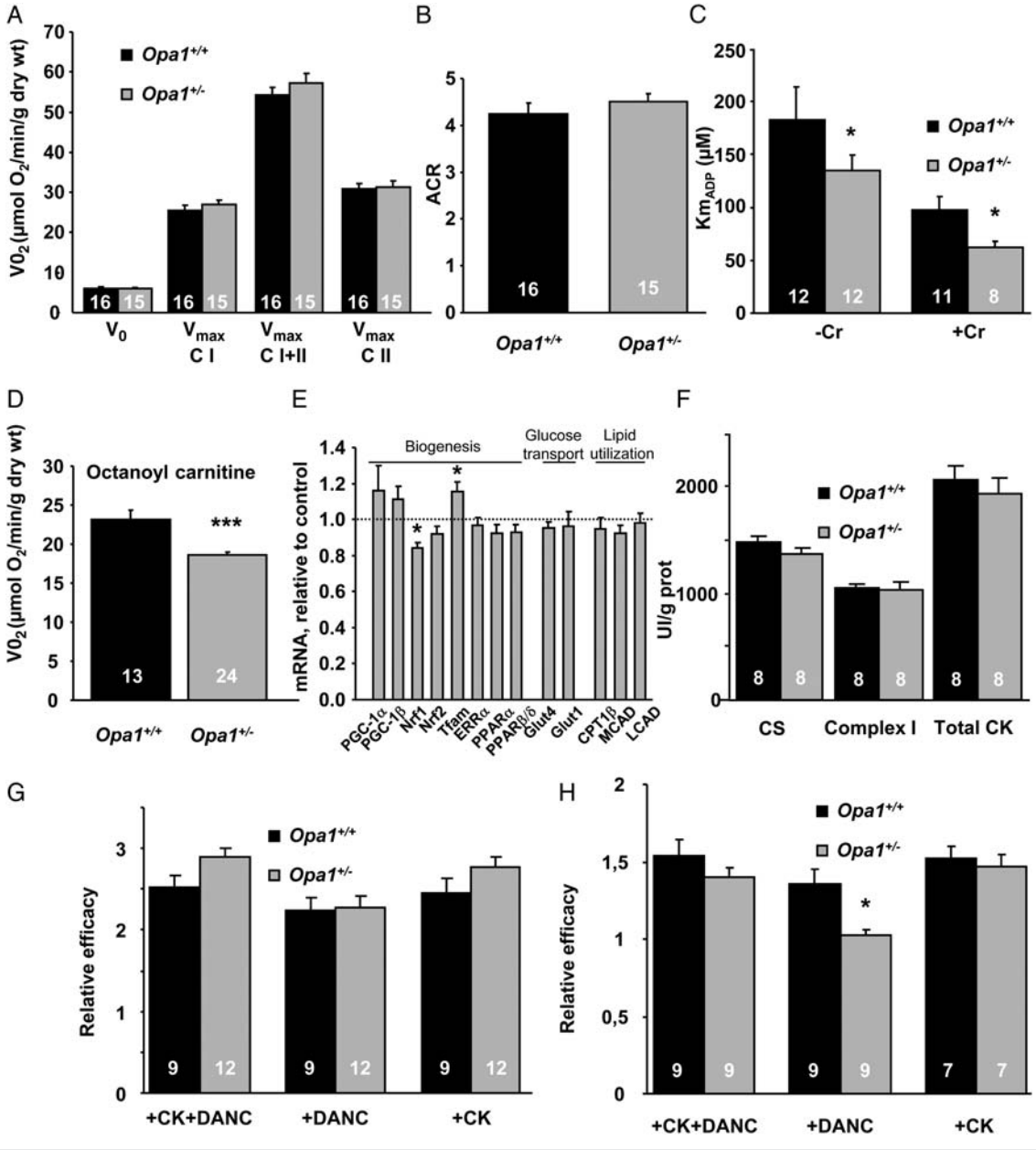

Figure 4 Cardiac energy metabolism of *Opa1*$^{+/+}$ and *Opa1*$^{+/-}$ mice. (*A*) Oxygen consumption rate of skinned ventricular fibres in the absence (V_0) or presence of 2 mM ADP (V_{max}) with 10 mM glutamate and 4 mM malate (complex I, CI), 15 mM succinate (both CI and complex II CI + II), and after complex I inhibition with 2 mM amytal (CII). (*B*) Acceptor control ratio. (*C*) Apparent K_m of oxygen consumption for ADP with (+Cr) or without (−Cr) 12 mM creatine. (*D*) Oxygen consumption rate with 2 mM ADP and 4 mM malate and 0.1 mM octanoyl carnitine. (*E*) mRNA levels of proteins involved in mitochondrial biogenesis, glucose transport, and lipid utilization. (*F*) Citrate synthase (CS), complex I and total creatine kinase (CK) activities. (*G* and *H*) Efficacy of CK and mitochondria (DANC) to support SERCA (*G*) or myosin ATPase (*H*) in permeabilized fibres. *$P < 0.05$ vs. *OPA1*$^{+/+}$ ***$P < 0.001$ vs. *OPA1*$^{+/+}$.

sections confirmed that there was also no apparent change in SR mitochondrial contacts (Supplementary material online, *Figure S5*).

The ability of these different energetic systems to support myosin-ATPase activity was then assessed by measuring the rigour tension developed by permeabilized fibres when the MgATP concentration was progressively decreased. The ability of DANC plus CK or CK alone to provide a high ATP/ADP ratio in the myofibrillar compartment was similar for the two groups (*Figure 4H*). However, DANC in *Opa1*$^{+/-}$ mice was significantly less efficient than in *Opa1*$^{+/+}$ mice: in *Opa1*$^{+/+}$ fibres, working mitochondria shifted $pMgATP_{50}$ for rigour by 1.36 ± 0.09 units, whereas, in Opa1$^{+/-}$ fibres, this parameter was as low as 1.03 ± 0.04 ($P < 0.01$). This showed that direct adenine nucleotide channelling from mitochondria to myosin ATPase was altered in hearts of *Opa1*$^{+/-}$ mice.

3.4 Mitochondrial Ca^{2+} retention capacity and permeability transition pore properties

The impact of partial Opa1 deficiency on the mitochondrial calcium retention capacity (CRC) and the PTP state was assessed *in situ* in

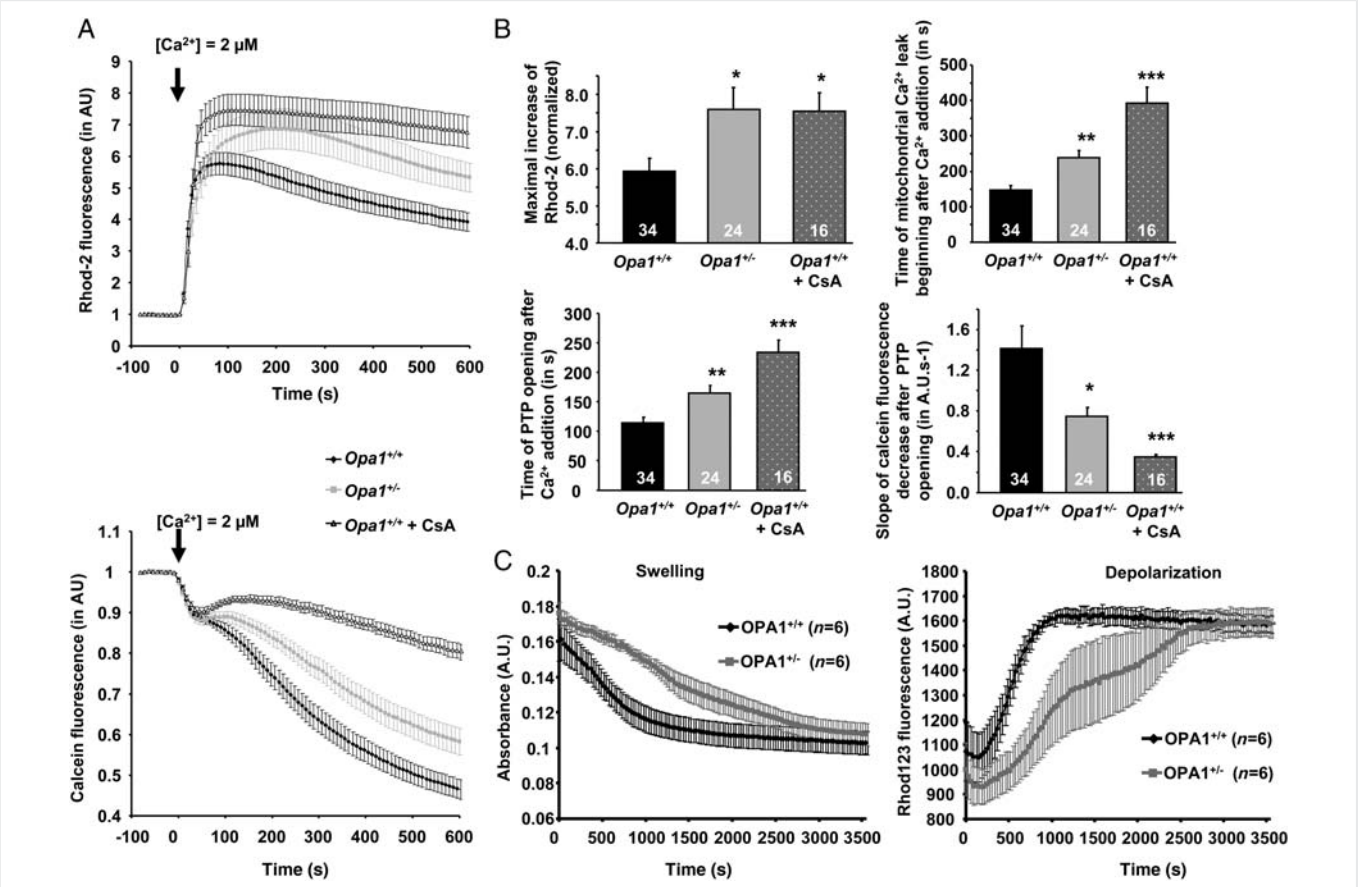

Figure 5 Kinetics of mitochondrial calcium loading and PTP opening in permeabilized cardiomyocytes and isolated mitochondria of *Opa1*$^{+/+}$ and *Opa1*$^{+/-}$ mice. (*A*) Upper panel: time course of mitochondrial calcium accumulation following Ca^{2+} addition (indicated by arrow) measured by Rhod-2 fluorescence. Lower panel: time course of mitochondrial calcein fluorescence following Ca^{2+} addition (indicated by arrow). (*B*) Mean values of mitochondrial calcium loading capacity and PTP opening properties**.** Upper panel, maximal increase of Rhod-2 fluorescence (left panel) and time to the beginning of mitochondrial Ca^{2+} leak after Ca^{2+} addition (right panel)**.** Lower panel, time to PTP opening after Ca^{2+} addition (left panel), and slope of calcein fluorescence decrease after PTP opening (right panel). *$P < 0.05$; **$P < 0.01$; ***$P < 0.001$ vs. *Opa1*$^{+/+}$. (*C*) Time course of swelling (left) and depolarization (right) of isolated mitochondria after addition of 25 µM Ca^{2+}.

permeabilized cardiomyocytes by fluorescence techniques. Following addition of 2 µM calcium, intra-mitochondrial [Ca^{2+}] progressively increased, as indicated by the rise in Rhod-2 fluorescence, until PTP opening-induced calcium loss from the mitochondrial matrix (*Figure 5A*, upper panel). Similarly, PTP opening provoked the release of intra-mitochondrial calcein, which induced a decrease in calcein fluorescence (*Figure 5A*, lower panel). The addition of cyclosporin A greatly reduced the leakage of calcein and Rhod-2 fluorescence, confirming that the observed phenomenon was indeed PTP opening. In comparison with *Opa1*$^{+/+}$ cardiomyocytes, *Opa1*$^{+/-}$ cells loaded more calcium and PTP opening was delayed (*Figure 5A* and *B*). Statistical analysis demonstrated a significant increase in mitochondrial CRC in *Opa1*$^{+/-}$ cardiomyocytes and, consequently, a shift in the onset of Ca^{2+} leakage from mitochondria (*Figure 5B*, upper panel), suggesting a change in the probability of PTP opening. This finding was confirmed by the analysis of calcein traces, which showed a delay in calcein leak and PTP opening, as well as a decrease in the rate of calcein leak in *Opa1*$^{+/-}$ cardiomyocytes (*Figure 5B*, lower panel). These results demonstrated a link between mutation in *Opa1* and changes in mitochondrial PTP function and mitochondrial CRC.

We confirmed these results using isolated mitochondria (*Figure 5C*). Swelling and depolarization of mitochondria were monitored after addition of 25 µM Ca^{2+}. We observed no difference in the resting membrane potential, as assessed by Rhod123 fluorescence. Furthermore, after Ca^{2+} the addition of, as in isolated permeabilized cardiomyocytes, a delay in the opening of mPTP in *Opa1*$^{+/-}$ *mice* was observed. Indeed, $t_{1/2}$ for depolarization and swelling curves were 8.7 ± 0.7 and 10.4 ± 0.8 min, respectively, in *Opa1*$^{+/+}$, but increased to 22.0 ± 4.7 and 24.0 ± 4.4 min in *Opa1*$^{+/-}$ *mice* ($P < 0.05$). Thus, the modifications of PTP function were intrinsically linked to the lack of OPA1 in mitochondria.

3.5 Myocardial hypertrophy and myocardial dysfunction induced by pressure overload

To estimate the role of OPA1 in cardiac response to mechanical stress and to unmask possible loss in functional reserve, we

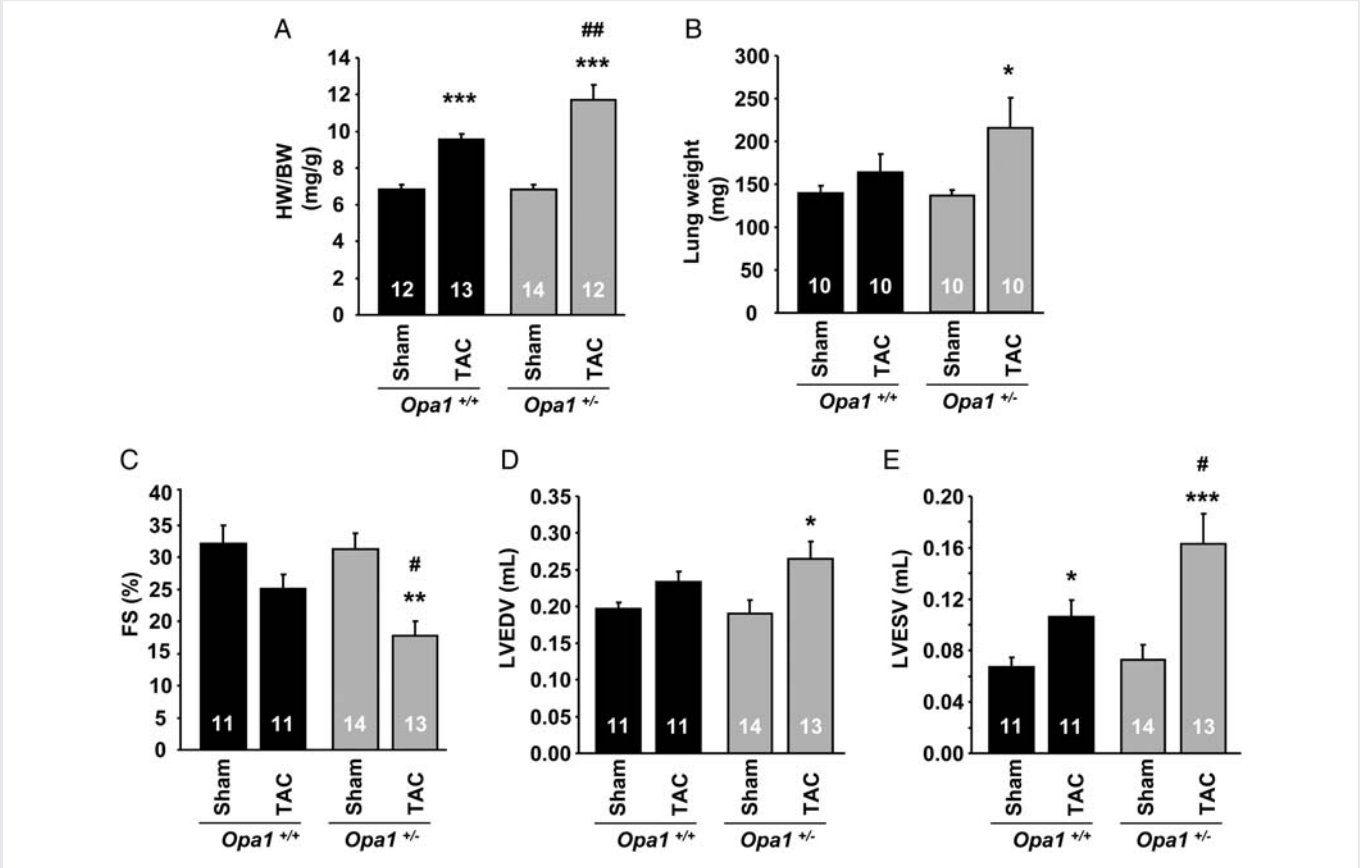

Figure 6 Anatomical characteristics and echocardiographic data of $Opa1^{+/-}$ mice following transverse aortic constriction (TAC). (*A*) Heart weight to body weight ratio. (*B*) Lung weight. (*C*) Fractional shortening. (*D*) Left ventricular end-diastolic diameter. (*E*) Left ventricle end-systolic volume. $^{*}P < 0.05$; $^{**}P < 0.01$; $^{***}P < 0.001$ vs. sham. $^{\#}P < 0.05$; $^{\#\#}P < 0.01$ vs. $Opa1^{+/+}$-TAC.

performed echocardiographic analysis 6 weeks after TAC. In both sham groups ($Opa1^{+/+}$-sham and $Opa1^{+/-}$-sham), the heart weight/body weight ratio (*Figure 6A*) and parameters of the cardiac function (*Figure 6C–E*) were similar. On the other hand, hearts from $Opa1^{+/-}$-TAC mice showed an almost two-fold greater hypertrophy (+72%) than did $Opa1^{+/+}$-TAC (+40%) (*Figure 6A*). The high level of hypertrophy was associated with significant alterations of cardiac function. In contrast to $Opa1^{+/+}$ hearts where TAC did not induce significant changes in the contractile indices (except in LV end-systolic volume), in the $Opa1^{+/-}$ group, TAC led to significant ventricular dilation, as shown by the increase in LV end-diastolic volume and ventricular dysfunction, evidenced by a decrease in end-systolic volume, and a 43% reduction in left ventricle FS (*Figure 6C–E*). The cardiac output index was also calculated, but no significant difference between groups was observed ($Opa1^{+/+}$-sham: 2.18 ± 0.23; $Opa1^{+/+}$-TAC: 2.12 ± 0.18; $Opa1^{+/-}$-sham: 1.99 ± 0.13; $Opa1^{+/-}$-TAC: 1.87 ± 0.17 mL/min/g). Indices of heart failure, such as pulmonary oedema, tended to appear in $Opa1^{+/-}$ mice (*Figure 6B*). As expected, markers of mitochondrial content or biogenesis (Supplementary material online, *Table S2*) were down-regulated, and markers of stress or fibrosis (Supplementary material online, *Figure S6*) were up-regulated by TAC, but no marked difference was observed between $Opa1^{+/-}$ and $Opa1^{+/+}$ mice. Taken together, this suggests that the heart of $Opa1^{+/-}$ mice have an increased sensitivity to mechanical stress.

4. Discussion

The role of OPA1 in the heart has been poorly explored, despite the high expression level of OPA1 and other dynamin-related proteins (DRPs) in this organ.[15–17,26–29] Adult cardiomyocytes are highly oxidative cells and possess a large amount of mitochondria. However, a fast dynamic of these organelles was not clearly demonstrated.[27] Obviously, this does not mean that DRPs are silent in the adult heart and/or have no important physiological roles in this organ. We thus investigated the consequences of the decreased OPA1 expression on the intracellular energetic pathways and mouse heart function. The present results show that, (i) OPA1 depletion induced mitochondrial network remodelling, while (ii) oxidative capacity and respiratory chain function were not altered, but (iii) direct channelling of ATP and ADP between mitochondria and myosin ATPases was reduced in mutant mice, and (iv) mitochondria of $Opa1^{+/-}$ mice accumulated more calcium and presented a delay in calcium-induced PTP opening, and finally (v) despite a normal cardiac function at basal state, the mutant mice were more sensitive to prolonged haemodynamic stress.

OPA1 down-regulation induced clear changes in mitochondrial morphology and cytoarchitecture. Indeed, in accordance with roles already attributed to OPA1,[30] we observed alterations of the mitochondrial cristae. However, unexpectedly, we observed heterogeneity in the mitochondrial size with the appearance of larger mitochondria

in *Opa1*$^{+/-}$ cardiomyocytes. Although modifications of the mitochondrial network were expected, these results are surprising because several previous studies had shown that the down-regulation of proteins involved in fusion induces fragmentation of the mitochondria.[31–33] However, our results are consistent with a recent study, showing that while Mfn2 KO mice exhibit mitochondrial fragmentation in neonatal cardiomyocytes, the opposite result, i.e. larger mitochondria, was observed in adult myocardium.[29] Thus, our results can be explained by the specific architectural constraints of the adult cardiomyocyte that limit mitochondrial movements in contrast to neonatal cardiac cells. Indeed, the adult cardiac cell is a paradigm of highly compartmentalized cells possessing a sophisticated subcellular architecture in which repeated arrays of sarcomeres, T-tubules, SR, and mitochondria interact. Therefore, it appears that a deficit in fusion protein may result in incomplete fusion in a complex cell type such as the adult cardiomyocyte, and in fragmentation in a simpler cell model. It can be proposed that, in a constrained environment, a deficit in OPA1, by impairing fusion of inner mitochondrial membranes, would compromise further fission mechanisms.

A primary consequence of mitochondrial morphology alterations was a decrease in the K_m for ADP in *Opa1*$^{+/-}$ mice, which could result from disturbances in the cell architecture,[34] leading to weaker interactions between mitochondria and the surrounding organelles, such that mitochondria are more open to the cytosol.[10] A second consequence is an impairment of energy transfer between mitochondria and myofilaments.[9,11] Indeed, our results show, for the first time, that a mere perturbation of the mitochondrial morphology may impair adenine nucleotide compartmentation, thereby confirming a link between cellular architecture and energy fluxes.[10,11] In the heart, the local energy-providing systems (DANC and CK) are redundant and therefore alterations in DANC have no major impact on basal cardiac function.[9] However, under conditions of chronic stress, deficient energy transfer may have a deleterious impact on cardiac function.[10,23]

In the heart of *Opa1*$^{+/-}$ mice, mitochondrial oxidative capacities and respiratory chain complexes were not changed. Similarly, in leucocytes from ADOA patients, which exhibit only a partial loss of OPA1 expression, no alteration in mitochondrial oxidative capacity was observed.[35] However, almost complete loss of OPA1 resulted in severely altered mitochondrial respiration.[36] The only change in metabolic phenotype found in the present study was an alteration of free fatty acid utilization by mitochondria. The mechanism responsible for this alteration is not clear. β-Oxidation does not seem to be involved because MCAD or LCAD RNAs were not modified. One can hypothesize that lack of OPA1 could disturb the organization of mitochondrial inner membranes and thus affect the transport of free fatty acids in the matrix. Alternatively, mitochondrial Ca^{2+} flux modifications, due to altered PTP properties (see below), can also affect metabolic substrate utilization.[37]

The most unexpected effect of OPA1 deficiency is related to PTP function and the mitochondrial CRC. Using Rhod-2 and calcein, we observed higher CRC and a delayed PTP opening under calcium stimulation. Interestingly, *Mfn2* KO mice presented the same characteristics[29] suggesting a link between PTP function and DRPs. Various hypotheses can be proposed to explain how OPA1 can influence PTP function and enhance the capacity for Ca^{2+} retention. Firstly, because mitochondria from *Opa1*$^{+/-}$ mice are larger, they could, in principle, load more calcium,[28,38,39] but recent results suggest that a direct relationship between mitochondrial volume and the Ca^{2+} uptake capacity is unlikely.[29] Secondly, because OPA1 is located in the inner mitochondrial membrane and participates in the organization of mitochondrial cristae,[30] loss of this protein could disorganize the environment of the inter-membrane space and disturb the downstream signalling events.[3,40] In this regard, the PTP, which needs the proximity of the mitochondrial internal and external membranes to form, could be sensitive to OPA1 deletion and cristae disorganization. Finally, one cannot exclude that, due to its location, OPA1 could be a structural part of the supramolecular complex that forms the PTP.

A higher CRC and delayed PTP opening have been described as a cardioprotective mechanism against ischaemia/reperfusion injury.[28,29] However, we hypothesize that, in our model, these mitochondrial characteristics can be detrimental to the heart. Indeed, the TAC-induced haemodynamic stress resulted in greater cardiac hypertrophy and chamber dilation, and lower FS in *Opa1*$^{+/-}$ mice. In both strains at this stage; however, the cardiac output index was still maintained due to the chamber enlargement. One possible explanation for the increased remodelling in *Opa1*$^{+/-}$ mice is the lower sensitivity of PTP to calcium accumulation in the mitochondrial matrix, which could induce mitochondrial calcium overload. Indeed, it has suggested that higher intra-mitochondrial calcium content would reduce the metabolic reserve capacity of the heart.[37] Another possibility could be the partial loss of DANC efficacy found in our study. Finally, it is reasonable to suggest that the impairment of the mitochondrial dynamics does not allow an appropriate and homogeneous adaptation of the mitochondrial network to the increase in the energetic demand of stress, thereby exacerbating cardiac remodelling.

OPA1 has been proposed to be involved in the organization of cristae, and its deletion could modify the propensity of mitochondria to release cytochrome *c*. However, the correlation between the PTP, the morphology of cristae and the release of cytochrome *c*, is not straightforward.[41] Further experiments are needed to address this important issue.

In conclusion, we have established that the decreased expression of the OPA1 protein in a mouse model mimicking human ADOA disease has consequences for the morphology of mitochondria and for energetic transfers between organelles, as well as for mitochondrial CRC and PTP properties. These alterations could explain the sensitization of the heart to haemodynamic stress and show that OPA1 plays an important role in cardiac physiology.

Supplementary material

Supplementary material is available at *Cardiovascular Research* online.

Acknowledgements

We thank Dr R. Fischmeister for continuous support. We thank Eric Jacquet and Romain Barbet for TDLA analysis (IMAGIF qPCR-Platform, UPR-2301 CNRS Gif/Yvette). We also thank Valérie Domergue-Dupont and the animal core facility of IFR141 for efficient handling and preparation of the animals. We are grateful to Bernd Wissinger (Genetics Laboratory, Institute for Ophthalmic Research, Centre for Ophthalmology, University of Tübingen, Germany) for sharing the *Opa1*$^{+/-}$ mouse line.

Conflict of interest: none declared.

Funding

This work was partly supported by a grant VEGA 2/0116/12. This work was supported by grants from the European Union contract LSHM-CT-2005-018833/EUGeneHeart and a grant from University of Paris Sud (Attractivité). R.V.-C., C.B., and F.J. are scientists at Centre National de la Recherche Scientifique.

References

1. Liesa M, Palacin M, Zorzano A. Mitochondrial dynamics in mammalian health and disease. *Physiol Rev* 2009;**89**:799–845.
2. Legros F, Lombes A, Frachon P, Rojo M. Mitochondrial fusion in human cells is efficient, requires the inner membrane potential, and is mediated by mitofusins. *Mol Biol Cell* 2002;**13**:4343–4354.
3. Olichon A, Emorine LJ, Descoins E, Pelloquin L, Brichese L, Gas N *et al*. The human dynamin-related protein OPA1 is anchored to the mitochondrial inner membrane facing the inter-membrane space. *FEBS Lett* 2002;**523**:171–176.
4. Alexander C, Votruba M, Pesch UE, Thiselton DL, Mayer S, Moore A *et al*. OPA1, encoding a dynamin-related GTPase, is mutated in autosomal dominant optic atrophy linked to chromosome 3q28. *Nat Genet* 2000;**26**:211–215.
5. Delettre C, Lenaers G, Griffoin JM, Gigarel N, Lorenzo C, Belenguer P *et al*. Nuclear gene OPA1, encoding a mitochondrial dynamin-related protein, is mutated in dominant optic atrophy. *Nat Genet* 2000;**26**:207–210.
6. Zuchner S, Mersiyanova IV, Muglia M, Bissar-Tadmouri N, Rochelle J, Dadali EL *et al*. Mutations in the mitochondrial GTPase mitofusin 2 cause Charcot-Marie-Tooth neuropathy type 2A. *Nat Genet* 2004;**36**:449–451.
7. Votruba M, Moore AT, Bhattacharya SS. Clinical features, molecular genetics, and pathophysiology of dominant optic atrophy. *J Med Genet* 1998;**35**:793–800.
8. Delettre C, Griffoin JM, Kaplan J, Dollfus H, Lorenz B, Faivre L *et al*. Mutation spectrum and splicing variants in the OPA1 gene. *Hum Genet* 2001;**109**:584–591.
9. Kaasik A, Veksler V, Boehm E, Novotova M, Minajeva A, Ventura-Clapier R. Energetic crosstalk between organelles: architectural integration of energy production and utilization. *Circ Res* 2001;**89**:153–159.
10. Wilding JR, Joubert F, de Araujo C, Fortin D, Novotova M, Veksler V *et al*. Altered energy transfer from mitochondria to sarcoplasmic reticulum after cytoarchitectural perturbations in mice hearts. *J Physiol* 2006;**575**:191–200.
11. Piquereau J, Novotova M, Fortin D, Garnier A, Ventura-Clapier R, Veksler V *et al*. Postnatal development of mouse heart: formation of energetic microdomains. *J Physiol* 2010;**588**:2443–2454.
12. Ventura-Clapier R, Garnier A, Veksler V. Energy metabolism in heart failure. *J Physiol* 2004;**555**:1–13.
13. Ventura-Clapier R, Garnier A, Veksler V, Joubert F. Bioenergetics of the failing heart. *Biochim Biophys Acta* 2011;**1813**:1360–1372.
14. Ong SB, Hausenloy DJ. Mitochondrial morphology and cardiovascular disease. *Cardiovasc Res* 2010;**88**:16–29.
15. Shahrestani P, Leung HT, Le PK, Pak WL, Tse S, Ocorr K *et al*. Heterozygous mutation of *Drosophila* Opa1 causes the development of multiple organ abnormalities in an age-dependent and organ-specific manner. *PLoS One* 2009;**4**:e6867.
16. Dorn GW II, Clark CF, Eschenbacher WH, Kang MY, Engelhard JT, Warner SJ *et al*. MARF and Opa1 control mitochondrial and cardiac function in *Drosophila*. *Circ Res* 2011;**108**:12–17.
17. Chen L, Gong Q, Stice JP, Knowlton AA. Mitochondrial OPA1, apoptosis, and heart failure. *Cardiovasc Res* 2009;**84**:91–99.
18. Alavi MV, Bette S, Schimpf S, Schuettauf F, Schraermeyer U, Wehrl HF *et al*. A splice site mutation in the murine Opa1 gene features pathology of autosomal dominant optic atrophy. *Brain* 2007;**130**:1029–1042.
19. Alavi MV, Fuhrmann N, Nguyen HP, Yu-Wai-Man P, Heiduschka P, Chinnery PF *et al*. Subtle neurological and metabolic abnormalities in an Opa1 mouse model of autosomal dominant optic atrophy. *Exp Neurol* 2009;**220**:404–409.
20. Heiduschka P, Schnichels S, Fuhrmann N, Hofmeister S, Schraermeyer U, Wissinger B *et al*. Electrophysiological and histologic assessment of retinal ganglion cell fate in a mouse model for OPA1-associated autosomal dominant optic atrophy. *Invest Ophthalmol Vis Sci* 2010;**51**:1424–1431.
21. Verde I, Vandecasteele G, Lezoualc'h F, Fischmeister R. Characterization of the cyclic nucleotide phosphodiesterase subtypes involved in the regulation of the L-type Ca^{2+} current in rat ventricular myocytes. *Br J Pharmacol* 1999;**127**:65–74.
22. Kuznetsov AV, Veksler V, Gellerich FN, Saks V, Margreiter R, Kunz WS. Analysis of mitochondrial function *in situ* in permeabilized muscle fibers, tissues and cells. *Nat Protoc* 2008;**3**:965–976.
23. Joubert F, Wilding JR, Fortin D, Domergue-Dupont V, Novotova M, Ventura-Clapier R *et al*. Local energetic regulation of sarcoplasmic and myosin ATPase is differently impaired in rats with heart failure. *J Physiol* 2008;**586**:5181–5192.
24. Palmer JW, Tandler B, Hoppel CL. Biochemical properties of subsarcolemmal and interfibrillar mitochondria isolated from rat cardiac muscle. *J Biol Chem* 1977;**252**:8731–8739.
25. Belzacq-Casagrande AS, Martel C, Pertuiset C, Borgne-Sanchez A, Jacotot E, Brenner C. Pharmacological screening and enzymatic assays for apoptosis. *Front Biosci* 2009;**14**:3550–3562.
26. Fang L, Moore XL, Gao XM, Dart AM, Lim YL, Du XJ. Down-regulation of mitofusin-2 expression in cardiac hypertrophy *in vitro* and *in vivo*. *Life Sci* 2007;**80**:2154–2160.
27. Beraud N, Pelloux S, Usson Y, Kuznetsov AV, Ronot X, Tourneur Y *et al*. Mitochondrial dynamics in heart cells: very low amplitude high frequency fluctuations in adult cardiomyocytes and flow motion in non beating Hl-1 cells. *J Bioenerg Biomembr* 2009;**41**:195–214.
28. Ong SB, Subrayan S, Lim SY, Yellon DM, Davidson SM, Hausenloy DJ. Inhibiting mitochondrial fission protects the heart against ischemia/reperfusion injury. *Circulation* 2010;**121**:2012–2022.
29. Papanicolaou KN, Khairallah RJ, Ngoh GA, Chikando A, Luptak I, O'Shea KM *et al*. Mitofusin-2 maintains mitochondrial structure and contributes to stress-induced permeability transition in cardiac myocytes. *Mol Cell Biol* 2011;**31**:1309–1328.
30. Frezza C, Cipolat S, Martins de Brito O, Micaroni M, Beznoussenko GV, Rudka T *et al*. OPA1 controls apoptotic cristae remodeling independently from mitochondrial fusion. *Cell* 2006;**126**:177–189.
31. Chen H, Detmer SA, Ewald AJ, Griffin EE, Fraser SE, Chan DC. Mitofusins Mfn1 and Mfn2 coordinately regulate mitochondrial fusion and are essential for embryonic development. *J Cell Biol* 2003;**160**:189–200.
32. Cipolat S, Martins de Brito O, Dal Zilio B, Scorrano L. OPA1 requires mitofusin 1 to promote mitochondrial fusion. *Proc Natl Acad Sci U S A* 2004;**101**:15927–15932.
33. Olichon A, Baricault L, Gas N, Guillou E, Valette A, Belenguer P *et al*. Loss of OPA1 perturbates the mitochondrial inner membrane structure and integrity, leading to cytochrome c release and apoptosis. *J Biol Chem* 2003;**278**:7743–7746.
34. Saks V, Kuznetsov A, Andrienko T, Usson Y, Appaix F, Guerrero K *et al*. Heterogeneity of ADP diffusion and regulation of respiration in cardiac cells. *Biophys J* 2003;**84**:3436–3456.
35. Mayorov VI, Lowrey AJ, Biousse V, Newman NJ, Cline SD, Brown MD. Mitochondrial oxidative phosphorylation in autosomal dominant optic atrophy. *BMC Biochem* 2008;**9**:22.
36. Chen H, Chomyn A, Chan DC. Disruption of fusion results in mitochondrial heterogeneity and dysfunction. *J Biol Chem* 2005;**280**:26185–26192.
37. Elrod JW, Wong R, Mishra S, Vagnozzi RJ, Sakthievel B, Goonasekera SA *et al*. Cyclophilin D controls mitochondrial pore-dependent Ca(2+) exchange, metabolic flexibility, and propensity for heart failure in mice. *J Clin Invest* 2010;**120**:3680–3687.
38. Nogueira V, Devin A, Walter L, Rigoulet M, Leverve X, Fontaine E. Effects of decreasing mitochondrial volume on the regulation of the permeability transition pore. *J Bioenerg Biomembr* 2005;**37**:25–33.
39. Iijima T, Tanaka K, Matsubara S, Kawakami H, Mishima T, Suga K *et al*. Calcium loading capacity and morphological changes in mitochondria in an ischemic preconditioned model. *Neurosci Lett* 2008;**448**:268–272.
40. Wasilewski M, Scorrano L. The changing shape of mitochondrial apoptosis. *Trends Endocrinol Metab* 2009;**20**:287–294.
41. Sun MG, Williams J, Munoz-Pinedo C, Perkins GA, Brown JM, Ellisman MH *et al*. Correlated three-dimensional light and electron microscopy reveals transformation of mitochondria during apoptosis. *Nat Cell Biol* 2007;**9**:1057–1065.